Journal of Bacteriology

Bacteriology | Full-Length Text

Intracellular ATP concentration is a key regulator of bacterial cell fate

Bo Li,[1] Xiao Chen,[1] Jin-Yu Yang,[2] Song Gao,[2] Fan Bai[1]

AUTHOR AFFILIATIONS See affiliation list on p. 16.

ABSTRACT ATP, most widely known as the primary energy source for numerous cellular processes, also exhibits the characteristics of a biological hydrotrope. The viable but nonculturable (VBNC) and persister states are two prevalent dormant phenotypes employed by bacteria to survive challenging environments, both of which are associated with low metabolic activity. Here, we investigate the intracellular ATP concentration of individual VBNC and persister cells using a sensitive ATP biosensor QUEEN-7μ and reveal that both types of cells possess a lower intracellular ATP concentration than culturable and sensitive cells, although there is a certain overlap in the intracellular ATP concentrations between antibiotic-sensitive cells and persisters. Moreover, we successfully separated VBNC cells from culturable cells using fluorescence-activated cell sorting based on the intracellular ATP concentration threshold of 12.5 μM. Using an enriched VBNC cell population, we confirm that the precipitation of proteins involved in key biological processes promotes VBNC cell formation. Notably, using green light-illuminated proteorhodopsin (PR), we demonstrate that VBNC cells can be effectively resuscitated by elevating their intracellular ATP concentration. These findings highlight the crucial role of intracellular ATP concentration in the regulation of bacterial cell fate and provide new insights into the formation of VBNC and persister cells.

IMPORTANCE The viable but nonculturable (VBNC) and persister states are two dormant phenotypes employed by bacteria to counter stressful conditions and play a crucial role in chronic and recurrent bacterial infections. However, the lack of precise detection methods poses significant threats to public health. Our study reveals lower intracellular ATP concentrations in these states and establishes an ATP threshold for distinguishing VBNC from culturable cells. Remarkably, we revive VBNC cells by elevating their intracellular ATP levels. This echoes recent eukaryotic studies where modulating metabolism impacts outcomes like osteoarthritis treatment and lifespan extension in *Caenorhabditis elegans*. Our findings underscore the crucial role of intracellular ATP levels in governing bacterial fate, emphasizing ATP manipulation as a potential strategy to steer bacterial behavior.

KEYWORDS VBNC state, persister, intracellular ATP concentration, resuscitation

Bacteria employ sophisticated survival mechanisms to counter various stresses, including starvation, low temperature, acidity, UV exposure, and antibiotic treatment (1–4). In this context, two dormant phenotypes have been identified: the viable but nonculturable (VBNC) and persister states. VBNC cells typically refer to cells that do not proliferate on routine culture media but remain viable, infectious, and capable of becoming culturable upon resuscitation (5–7). During the formation of VBNC cells, bacteria undergo significant cellular changes, such as altered gene expression, reduced macromolecular synthesis, protein precipitation, energy depletion, and ion leakage (8–11). On the other hand, persisters represent a subpopulation of bacterial cells that are

Editor Mohamed Y. El-Naggar, University of Southern California, Los Angeles, California, USA

Address correspondence to Fan Bai, fbai@pku.edu.cn.

The authors declare no conflict of interest.

Received 11 May 2024
Accepted 29 September 2024
Published 12 November 2024

phenotypically tolerant to multiple antibiotics and play a crucial role in chronic and recurrent bacterial infections, such as tuberculosis (TB), Lyme disease, and urinary tract infections (12–14). During antibiotic treatment, persister cells enter a dormant state in which they temporarily cease to divide but can rapidly revert to active growth upon the removal of stressors. In contrast, VBNC cells are unable to divide on standard growth media even after stressors are removed, a characteristic that distinctly separates VBNC from persister cells (15). Previous studies have also suggested that factors such as slow growth, toxin-antitoxin modules like *hipBA*, and the ppGpp response are involved in persister formation (16–19). These two dormant states share many similarities: both VBNC and persister cells are characterized by low metabolic activity (18–20), which implies a close relationship between them (16, 21–24).

VBNC pathogenic bacteria pose a significant threat to both food safety and public health since they cannot be reliably detected through conventional testing methods and can be resuscitated under specific conditions (25). It has been demonstrated that treatment with various chemical and biological agents can promote VBNC resuscitation, including resuscitation-promoting proteins, quorum-sensing agents, and even co-incubation with amoeba (26–28). However, these resuscitation experiments were conducted under conditions where the growth of remaining culturable cells was not inhibited. The presence of even a few culturable cells could cause misinterpretation of results, posing a challenge to the performance of VBNC resuscitation experiments. Moreover, since the occurrence of VBNC and persister cells is asynchronous in individual cells, previous studies relying on population measurement have not been sensitive or accurate enough to detect subtle changes in a specific dormant state. The optimal approach to investigating individual VBNC and persister cells is to use single-cell time-lapse imaging for observation and cell state identification.

ATP is a critical energy source that engages in numerous cellular processes such as DNA replication, biosynthesis, protein assembly, and biochemical reactions, as well as being a regulatory molecule essential for protein phosphorylation (29). In addition to these well-known functions, ATP has also been reported to act as a biological hydrotrope (30) and can prevent the formation of, and dissolve, protein aggregates. Previous studies have demonstrated that ATP-dependent protein aggregation can regulate the depth of bacterial dormancy (18), and the appearance of *Staphylococcus aureus* persisters is also associated with ATP depletion (31). A reduced intracellular ATP concentration is a common feature of VBNC and persister cells; therefore, it is imperative to characterize the intracellular ATP levels in different cellular states to gain a deeper understanding of their formation.

In the present work, we employ the single-cell ratiometric ATP sensor QUEEN-7μ to directly assess the intracellular ATP concentration of individual bacterial cells. Through VBNC and persister identification via time-lapse imaging, we identify an intracellular ATP concentration threshold of 12.5 μM that effectively distinguishes VBNC cells from culturable cells. By utilizing fluorescence-activated cell sorting (FACS) based on intracellular ATP concentration, we successfully enrich the VBNC cell population for protein mass-spectrometry analysis, confirming that precipitation of proteins involved in key biological processes (BPs) promotes the formation of VBNC cells. Moreover, we show that increasing the intracellular ATP concentration effectively resuscitates VBNC cells.

RESULTS

Intracellular ATP levels are highly heterogeneous in late stationary-phase bacteria

We investigated the intracellular ATP concentration of VBNC and persister cells utilizing late stationary-phase *Escherichia coli* expressing QUEEN-7μ (32). QUEEN-7μ is a highly sensitive fluorescence biosensor specifically engineered for measuring intracellular ATP concentrations. It binds ATP with a dissociation constant (Kd) of 7.2 μM at 25°C, making it well-suited for detecting micromole ATP level (32). It has been reported that nutrient depletion resulting from prolonged culture drives a greater number of cells into VBNC

and persister states (18). The average intracellular ATP level of *E. coli* in the late stationary phase (24 h) was found to be less than 100 µM, which falls within the measurement range of QUEEN-7µ (32). First, to validate the applicability of QUEEN-7µ in our study, we monitored the ATP response of QUEEN-7µ both *in vitro* and *in vivo*. As shown in Fig. 1a, the *in vitro* excitation spectra of QUEEN-7µ at various ATP concentrations peaked at 405 and 488 nm, corresponding to the ATP-bound and ATP-free forms, respectively (33). The ratio of the fluorescence intensities of the peaks at 405 and 488 nm, denoted as Ratio (405ex/488ex) or simply Ratio, changed in response to ATP concentration. We constructed a response curve of the Ratio of purified QUEEN-7µ to ATP concentrations (Fig. 1b). At 25°C, the Kd of QUEEN-7µ from ATP, calculated according to the calibration curve, was 17.5 µM. This Kd value is slightly higher than that reported previously (32), which may be attributed to the use of different instruments and imaging parameters. Generally, the photostability of fluorescence proteins varies with excitation power (34). According to the previous study, QUEEN-7µ is sensitive to temperature; therefore, unless specifically indicated, our imaging experiments were performed at 25°C (32).

We then validated the response of QUEEN-7µ to ATP *in vivo* using standard ATP depletion and recovery treatments in a population measurement experiment. Fluorescence imaging revealed successful expression of QUEEN-7µ in *E. coli* cells (Fig. 1c). As

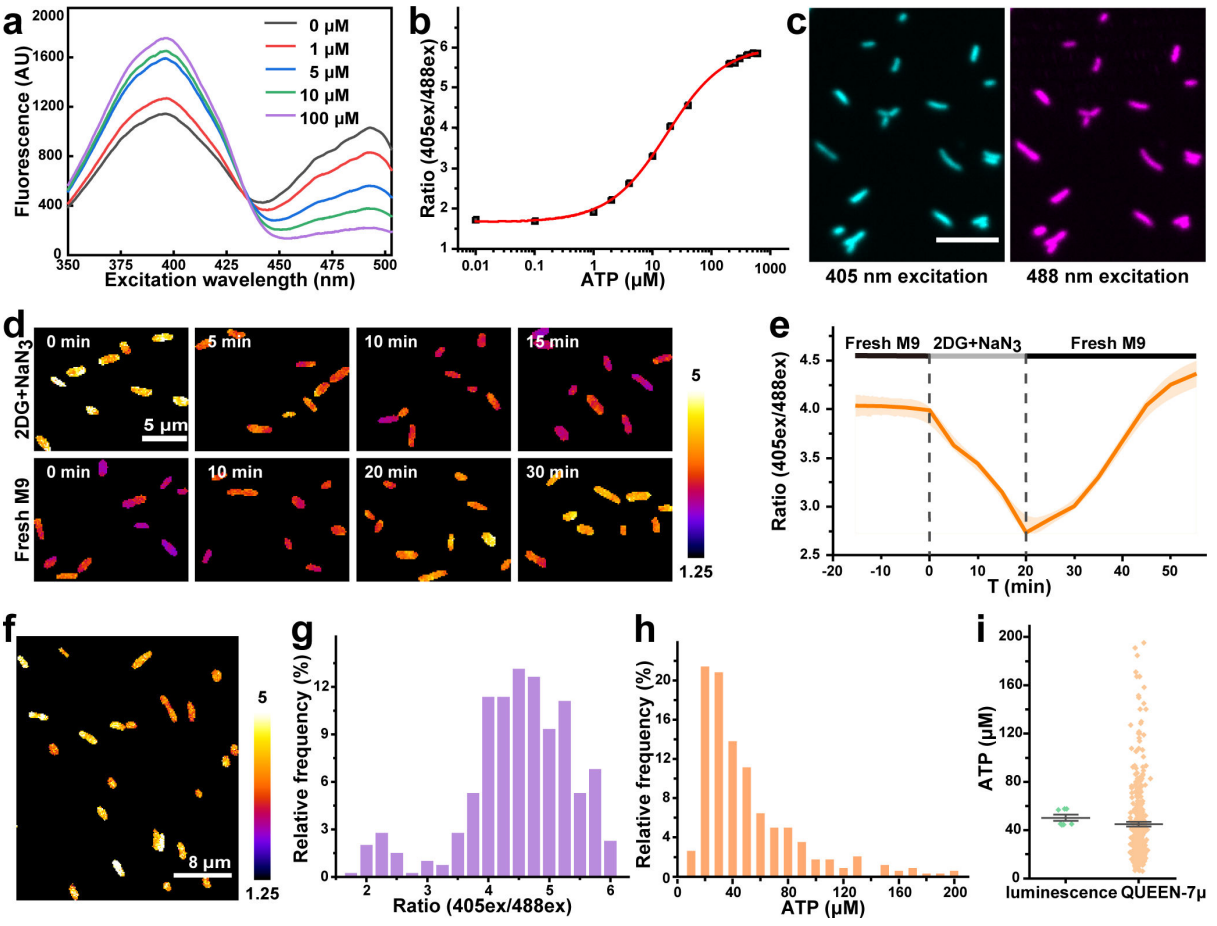

FIG 1 Estimation of the intracellular ATP concentration in late stationary-phase *E. coli* cells using QUEEN-7µ. (a) Excitation spectra of purified QUEEN-7µ at various ATP concentrations. (b) Ratio (405ex/488ex) of purified QUEEN-7µ in response to ATP concentration. (c) Representative fluorescence images of QUEEN-7µ cells at 24 h stationary culture. Scale bar, 10 µm. (d) Sequential images of the ratio of QUEEN-7µ cells at 24 h stationary culture after ATP depletion and M9 (1% glucose) recovery treatment. Scale bar, 5 µm. (e) Ratio of QUEEN-7µ cells in response to ATP depletion and subsequent M9 (1% glucose) recovery treatment. (f) Representative image of the Ratio of QUEEN-7µ cells at 24 h stationary culture. Scale bar, 8 µm. (g and h) Distribution of the Ratio and intracellular ATP concentration of QUEEN-7µ cells at 24 h stationary culture. (i) Intracellular ATP concentration of QUEEN-7µ cells at 24 h stationary culture as estimated by the luciferase assay and QUEEN-7µ (n = 469). The horizontal line represents the mean, and the whiskers represent the SEM. All experiments were performed at 25°C.

shown in Fig. 1d, the Ratio of QUEEN-7μ cells at 24 h stationary culture decreased rapidly following a 15 min exposure to the ATP depletion agents 2-deoxyglucose (2DG; 10 mM) and sodium azide (NaN_3; 10 mM). After the cells were washed and replenished with fresh M9 medium containing 1% glucose, the Ratio increased and recovered to its initial level within 20 min (Fig. 1e). To further validate the accuracy of intracellular ATP concentration measurement in late stationary-phase bacteria using QUEEN-7μ (Fig. 1f through h), we compared the results with those from the luciferase assay (Fig. 1i), which were similar (QUEEN-7μ, 45.0 ± 1.9 μM; luciferase assay, 50.2 ± 2.5 μM). At the single-cell level, the intracellular ATP concentration of QUEEN-7μ cells at 24 h stationary culture mainly ranged from several to 200 μM (Fig. 1h). Although a few cells exhibited ATP concentration exceeding 200 μM, considering the sensor's measurement is only reliable within the detection range of 1–200 μM, our analysis primarily focused on cells within this detection range. In summary, QUEEN-7μ enables single-cell measurement of the intracellular ATP concentration in late stationary-phase bacteria, validating its applicability for subsequent experiments.

A threshold of intracellular ATP concentration separates VBNC cells from culturable cells

Next, we investigated the intracellular ATP concentration of both VBNC and culturable cells from the late stationary phase culture. Specifically, we measured the Ratio of QUEEN-7μ expressed *E. coli* cells at 30 h stationary culture using high-throughput fluorescence microscopy (Fig. S1a and b). We then replenished the cells with fresh Luria-Bertani (LB) broth and monitored their resuscitation to determine their respective cell states (VBNC or culturable). Our observations reveal that a subset of cells resumed growth quickly, aligning with the conventional definition of culturable cells (Fig. 2a; Movie S1). By contrast, a considerable proportion of the remaining cells showed no sign of resuscitation (Fig. 2a; Movie S1) following the exclusion of dead cells via propidium iodide (PI) staining (Fig. S1a). In the present study, we classified cells that did not resuscitate within 16 h of LB culture under a microscope as VBNC cells (18). We further compared the proportions of culturable cells defined by microscopy observation with those from traditional plate cultivation. As shown in Fig. S2, the proportions were almost identical, supporting our definitions of VBNC and culturable cells in this experimental context.

After identifying VBNC and culturable cells, we proceeded to investigate their intracellular ATP concentrations and found that VBNC cells (16.1 ± 1.2 μM) had a significantly lower intracellular ATP concentration than culturable cells (55.8 ± 6.8 μM; Fig. 2b through d). Notably, the Ratios of all viable cells encompassing both VBNC and culturable cells, as depicted by the black line in Fig. 2c, exhibited a bimodal distribution. Specifically, the intracellular ATP concentrations of VBNC cells were all below 32.5 μM, while those of culturable cells were consistently above 12.5 μM (Fig. 2d). These observations suggest that when intracellular ATP concentrations drop below 12.5 μM, cells enter the VBNC state, while ATP concentrations exceeding 32.5 μM, cells are culturable. Therefore, an intracellular ATP concentration threshold of 12.5 μM can be used to distinguish VBNC cells from culturable cells.

We further investigated the intracellular ATP concentration of VBNC and culturable QUEEN-7μ cells formed under other stress conditions (including $CuSO_4$, citric acid, and cold shock treatment), and the results were consistent with our findings from prolonged culture. As shown in Fig. S3, the intracellular ATP concentration of VBNC cells was significantly lower than that of culturable cells under these stress conditions. The distribution of intracellular ATP concentrations also revealed that, at an intracellular ATP concentration below 12.5 μM, cells were in the VBNC state (Fig. S3j through l). The overlap in intracellular ATP concentration between the VBNC and culturable cells varied across stress conditions (Fig. S3m); however, the threshold of 12.5 μM to distinguish VBNC cells from culturable cells remained consistently valid. Our study uncovers an interesting relationship between cell state and intracellular ATP concentration.

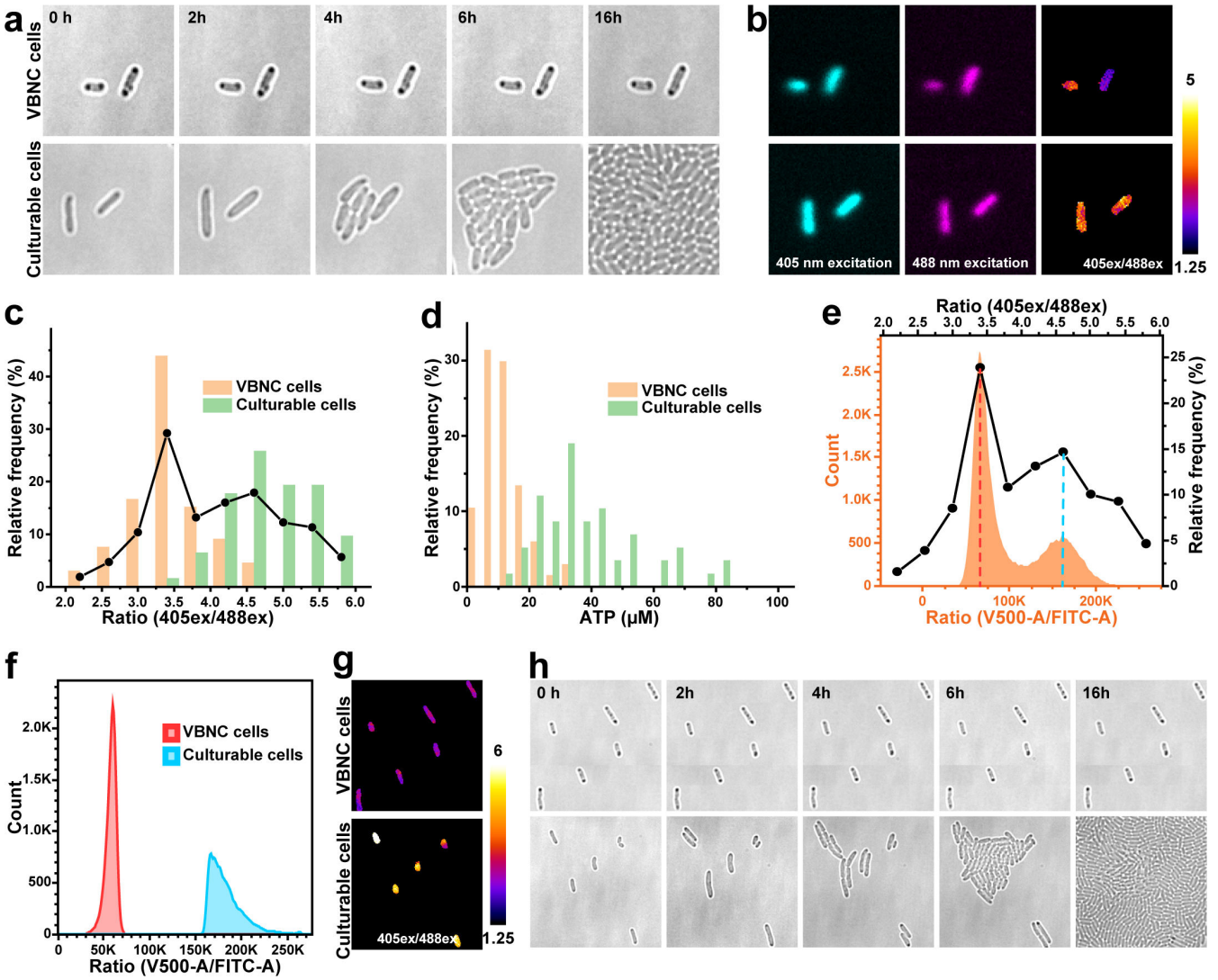

FIG 2 The intracellular ATP concentration of VBNC cells is significantly lower than culturable cells. (a) Time-lapse images of VBNC (upper) and culturable (lower) QUEEN-7μ cells incubated with fresh LB medium during resuscitation. Scale bar, 5 μm. (b) Fluorescence and ratio images of VBNC and culturable QUEEN-7μ cells before resuscitation, from the left panel. (c) Distribution of the Ratio of VBNC and culturable QUEEN-7μ cells at 30 h stationary culture. The black line represents the distribution of both VBNC and culturable cells. (d) Distribution of the intracellular ATP concentration of VBNC and culturable QUEEN-7μ cells at 30 h stationary culture. Data were obtained from 60 VBNC cells and 58 culturable cells. (e) Distributions of the ratio of QUEEN-7μ cells at 30 h stationary culture measured separately by microscopy (Ratio: V500-A/FITC-A in black) and FACS (Ratio: V500-A/FITC-A in orange). Both distributions are depicted as bimodal. (f) Distribution of the Ratio (V500-A/FITC-A) of VBNC and culturable QUEEN-7μ cells sorted by FACS. (g) Images of the Ratio (405ex/488ex) of VBNC and culturable QUEEN-7μ cells after FACS sorting from the right panel at 0 h. Scale bar, 5 μm. (h) Time-lapse images of the resuscitation of VBNC (upper) and culturable (lower) QUEEN-7μ cells sorted by FACS. Time-lapse images represent the same field of view over time.

Subsequently, we explored the possibility of separating VBNC cells from culturable cells in a bacterial population by FACS according to the intracellular ATP concentration. Figure 2e shows that the Ratio (405ex/488ex) obtained from QUEEN-7μ cells at 30 h stationary culture exhibited a bimodal distribution as captured by both FACS and fluorescence microscopy. To ensure comparability between the Ratios obtained from the different instruments, we aligned the peaks of their respective bimodal distributions. Our previous findings reveal that Ratios falling below 3.4 (corresponding to ATP <12.5 μM) indicated cells in the VBNC state, while Ratios surpassing 4.6 (corresponding to ATP >32.5 μM) highlighted cells in the culturable state. Consequently, when the Ratio measured by FACS was under 66 k (as indicated by the red dashed line), the cells were thought to be in the VBNC state, and when the Ratio exceeded 161 k (as indicated by the

blue dashed line), the cells were assumed to be in the culturable state. Subsequently, we employed a sequential gating strategy (Fig. S4) and FACS to sort VBNC and culturable cells based on the Ratio (Fig. 2f).

To evaluate the precision of FACS, we conducted resuscitation experiments for each cell group. As shown in Fig. 2g, the intracellular ATP concentration of sorted VBNC cells was significantly lower than that of sorted culturable cells. Notably, sorted VBNC cells showed no sign of resuscitation (Fig. 2h; Movie S2), while all sorted culturable cells were successfully revived during extended LB culture under a microscope (Fig. 2h; Movie S3). Additionally, the accuracy of VBNC cell sorting was confirmed to be 99% through conventional plate cultivation. In summary, these findings demonstrate that VBNC cells can be separated from culturable cells using FACS based on the intracellular ATP concentration.

Precipitation of proteins involved in key biological processes promotes VBNC cell formation

After the successful isolation of VBNC cells from culturable cells, we proceeded to investigate their proteome to gain further insights into the mechanism of VBNC cell formation. Under brightfield microscopy, we noticed that dark foci, demonstrated to be protein aggresomes (18), often accompanied VBNC cells but were not present in culturable cells (Fig. 3a). We then compared the soluble and precipitated insoluble proteomes between VBNC and culturable cells using total protein mass-spectrometry analysis (18), identifying 1,303 soluble and 1,406 insoluble proteins in VBNC cells, as well as 1,043 soluble and 1,109 insoluble proteins in culturable cells (Table S3). As shown in Fig. 3b, there were significant overlaps between the soluble and insoluble proteomes of VBNC and culturable cells. Moreover, the overlap was more pronounced in VBNC cells than in culturable cells, indicating that a greater number of proteins precipitated from the cytoplasm in VBNC cells. Consistent with this observation, the ratio of insoluble proteome abundance to total proteome abundance was notably higher in VBNC cells compared to culturable cells (Fig. 3c).

To further understand the manner by which protein precipitation influences the formation of VBNC cells, we investigated the proteins that were significantly increased in the insoluble fraction or significantly decreased in the soluble fraction in VBNC cells in comparison with culturable cells (Fig. 3d through i). The identification criteria were set at a threshold of ≥2 (≤ 0.5) based on the ratio of their relative amounts. In total, we identified 243 significantly increased insoluble proteins (increased insoluble proteome) and 192 significantly decreased soluble proteins (decreased soluble proteome) in VBNC cells (Table S3). The significantly increased insoluble proteins were found to be decreased within the soluble protein fraction in VBNC cells (Fig. S5), suggesting their precipitation from the cytoplasm. These results confirm that the formation of VBNC cells is accompanied by an increased level of protein precipitation.

We annotated these significantly precipitated proteins into three main gene ontology (GO) categories: BP, molecular function (MF), and cellular component (CC). The GO enrichment analysis of BP revealed that proteins associated with small molecule metabolic process, cellular amino acid metabolic process, and cellular detoxification were enriched in both the increased insoluble proteome and the decreased soluble proteome in VBNC cells, indicating their significant precipitation in VBNC cells (Fig. 3d, e and j). Additionally, energy metabolism-related proteins, such as those involved in the hexose metabolic process, alditol catabolic process, and polyol catabolic process, were also significantly enriched in the increased insoluble proteome in VBNC cells. The results for GO enrichment analysis of MF were consistent with those for the GO enrichment analysis of BP. As shown in Fig. 3f and g, the GO enrichment analysis of MF indicated that most of the significantly precipitated proteins were related to oxidoreductase activity, which is crucial in bioenergetic metabolic pathways. Additionally, proteins related to amino acid metabolism, such as endopeptidase activity, racemase and epimerase activity, transferase activity, and serine-type endopeptidase activity, were also enriched

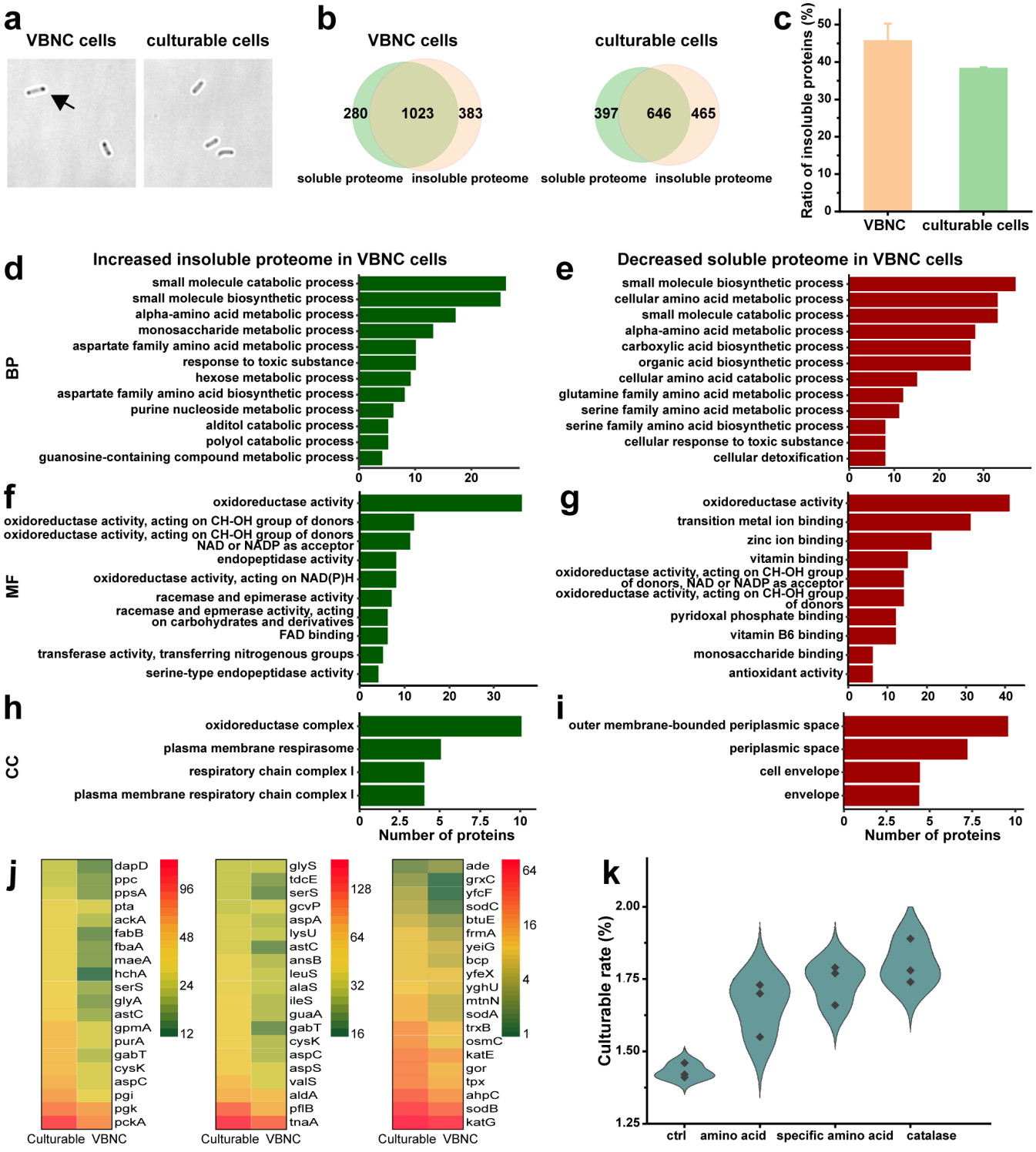

FIG 3 Protein precipitation is involved in VBNC cell formation. (a) Brightfield images of VBNC and culturable cells sorted by FACS. The arrow indicates a protein aggresome in the VBNC cell. Scale bar, 5 µm. (b) Venn diagram showing the overlap of the soluble and insoluble proteomes in VBNC and culturable cells. (c) The ratio of insoluble proteome abundance to total proteome abundance in VBNC and culturable cells. (d–i) Gene ontology (GO) enrichment analysis of the increased insoluble proteome (gene number = 243) and decreased soluble proteome (gene number = 192) in VBNC cells in comparison with culturable cells, including BP (d and e), molecular function (f and g), and cellular component (h and i). (j) Heatmaps showing the abundance of soluble proteins involved in key BPs, including small molecule catabolic process (left), cellular amino acid metabolic process (middle), and cellular response to toxic substance (right), in culturable and VBNC cells. The heatmap scale indicates protein abundance. (k) Resuscitation of FACS-sorted VBNC cells using amino acid and catalase supplements. Error bars indicate SEM.

in the increased insoluble proteome. Furthermore, the decreased soluble proteome in VBNC cells exhibited a significant enrichment in antioxidant activity. Taken together, these results suggest that proteins involved in metabolic activity, especially energy metabolism and cellular amino acid metabolism, as well as cellular detoxification or antioxidant activity, undergo significant precipitation during the formation of VBNC cells.

The GO enrichment analysis of CC revealed a significant enrichment of the oxidoreductase complex in the increased insoluble proteome and the cell envelope in the decreased soluble proteome, indicating a reduction in energy generation and destruction of cell envelope integrity in VBNC cells. Surprisingly, we also observed an increase in the abundance of certain proteins in the soluble fraction of VBNC cells compared to culturable cells (increased soluble proteome), with prominent examples being ribosomal subunit proteins rpoC, rpoB, ribonuclease R, and ribonuclease E (Table S3). Further investigation uncovered that proteins associated with RNA binding, ribosome biogenesis, ribosome assembly, ribosome binding, and ribosome subunit were significantly enriched in the increased soluble proteome (Fig. S6).

The precipitation of proteins involved in cellular amino acid metabolism, antioxidant activity, and energy metabolism may lead to amino acid deficiency, reactive oxygen species (ROS) accumulation, and ATP depletion in VBNC cells. To verify their impact on the formation of VBNC cells, we conducted resuscitation experiments using FACS-sorted VBNC cells supplemented with 1 × minimum essential medium (MEM) amino acids or a specific combination of amino acids (methionine, glutamine, threonine, serine, and asparagine) (35). Our results show that a limited number of VBNC cells were resuscitated, with the mean culturable ratio increasing by 0.23% and 0.31%, respectively (Fig. 3k). Additionally, we resuscitated VBNC cells by adding 5 U/μL antioxidant catalase (36), one of the main endogenous antioxidant enzymes that protect cells from oxidative damage by ROS (37), which resulted in a similar increase in the culturable ratio (0.37%). The resuscitation experiments were performed directly on LB agar plates to eliminate the potential influence of cell proliferation. These findings are consistent with previous studies reporting that amino acids and catalase promote the resuscitation of bacterial cells (35, 38). Taken together, our data suggest that while protein precipitation involved in key biological processes may promote the formation of VBNC cells, the direct causality and whether other factors play a role need further investigations.

An elevated intracellular ATP concentration facilitates the resuscitation of VBNC cells

Next, we conducted resuscitation experiments by elevating the intracellular ATP concentration. As mentioned previously, VBNC cells exhibit a significantly lower intracellular ATP concentration than culturable cells. To elevate the intracellular ATP concentration, we utilized proteorhodopsin (PR; Fig. S7), a light-powered proton pump endogenously expressed in marine bacteria (39). It has been demonstrated that light-activated PR-induced proton motive force can drive ATP synthesis (Fig. 4a) (40, 41). Under 10 mW green light illumination, we observed a significant increase in the Ratio of QUEEN-7μ-PR cells at 30 h stationary culture, while the Ratio remained unchanged without green light illumination (Fig. 4b and c). The mean cellular ATP concentration increased from 41 to 56 μM within 3 min of illumination, peaked at 68 μM after 9 min of illumination, and remained high under continuous illumination (Fig. 4d). These observations suggest that taking advantage of PR and green light illumination can rapidly elevate the intracellular ATP concentration in bacterial cells.

Our earlier results revealed an intracellular ATP concentration threshold that can be used to distinguish VBNC cells from culturable cells. Cells are considered culturable at an intracellular ATP concentration above 32.5 μM and VBNC at an intracellular ATP concentration below 12.5 μM. Interestingly, we observed that after 21 min of green light illumination, the proportion of cells with an intracellular ATP concentration exceeding 32.5 μM was significantly increased, while the proportion of cells with an intracellular ATP concentration below 12.5 μM was significantly decreased (Fig. 4e). This finding suggests

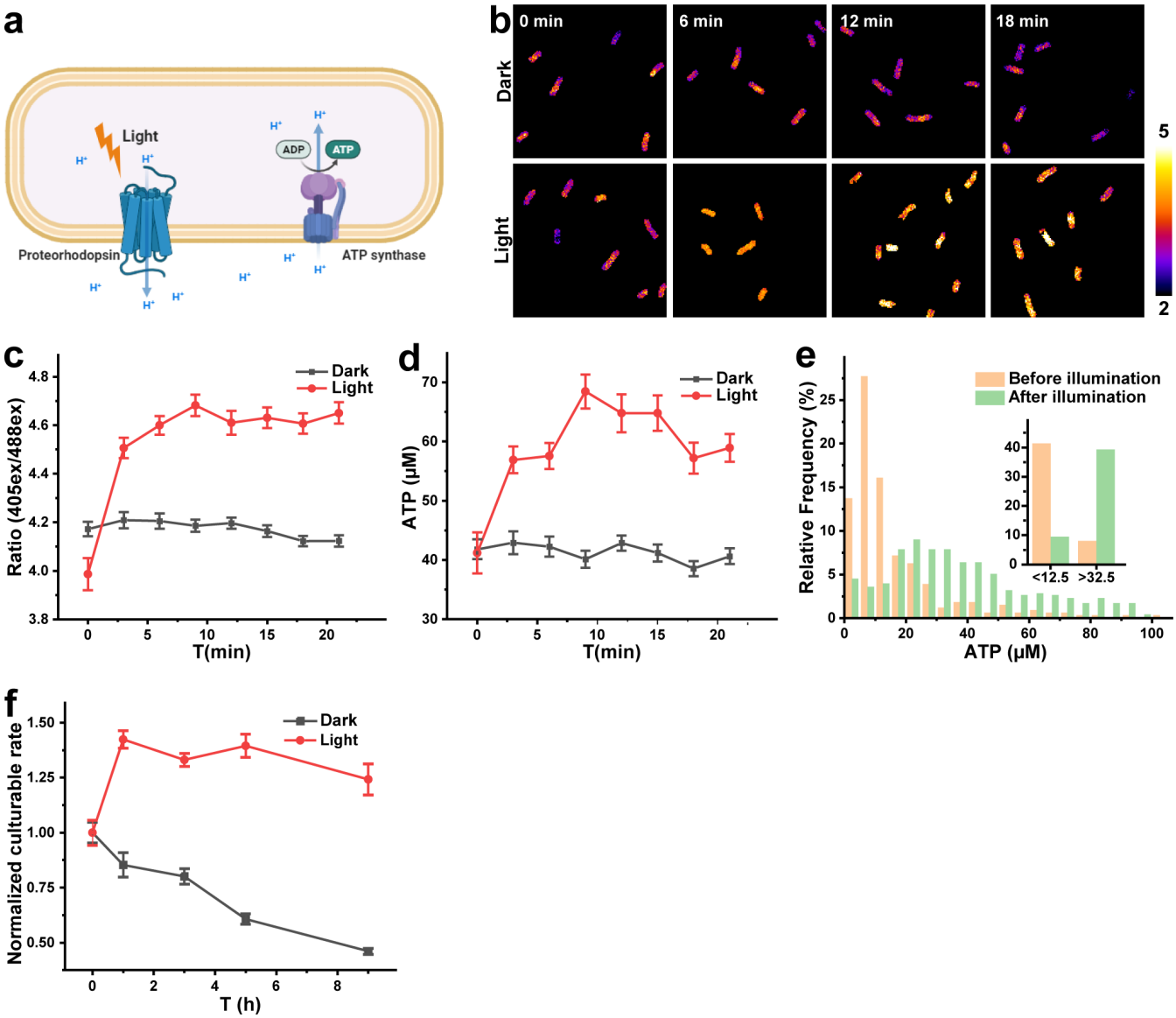

FIG 4 Increasing the intracellular ATP concentration promotes resuscitation of VBNC cells. (a) Schematic diagram illustrating the mechanism of PR-dependent ATP synthesis. (b) Sequential images of the Ratio of QUEEN-7μ-PR cells at 30 h stationary culture in the presence or absence of green light illumination. (c and d) The sequential mean Ratio and intracellular ATP concentration in QUEEN-7μ-PR cells at 30 h stationary culture in the presence or absence of green light illumination. (e) Distribution of the ATP concentration of QUEEN-7μ-PR cells at 30 h stationary culture prior to and following 21 min of green light illumination. (Inset) Comparison of the relative frequency of an intracellular ATP concentration lower than 12.5 μM and higher than 32.5 μM prior to and following green light illumination. (f) Culturability of QUEEN-7μ-PR cells at 30 h stationary culture in the presence or absence of green light illumination. Cells were incubated in phosphate-buffered saline (PBS) with exogenously added all-*trans* retinal. The normalized culturable rate is the ratio of the colony-formation unit (CFU) count after a certain incubation time to the mean CFU count after 1 h of incubation. All CFU experiments were performed in triplicate. All-*trans* retinal (20 μM) was added during cell culture. Error bars indicate SEM.

that some cells in the VBNC state may transform into the culturable state following elevation of their intracellular ATP concentration. To test this hypothesis, we conducted a resuscitation experiment in QUEEN-7μ-PR cells at 30 h stationary culture under green light illumination in nutrient-deficient phosphate-buffered saline (PBS). As shown in Fig. 4f, the normalized culturable rate was significantly increased by almost 40% following 2 h of green light illumination. Conversely, in the absence of green light illumination, the normalized culturable rate gradually decreased as cells transitioned from the culturable state into the VBNC state during culture in nutrient-deficient PBS. We also conducted a

resuscitation experiment with the cells cultured directly on LB plates and found that the normalized culturable rate increased by 11% after 8 h of green light illumination (Fig. S8). All-*trans* retinal (20 µM) was added during these resuscitation experiments. The reason that the resuscitation ratio for cells cultured on plates was lower than that for cells cultured in PBS may be the slow exchange rate of all-*trans* retinal on solid medium. Taken together, these results suggest that VBNC cells can be significantly resuscitated by elevating the intracellular ATP concentration via green light-illuminated PR.

The link between intracellular ATP concentration and antibiotic tolerance

We further explored the relationship between intracellular ATP concentration and bacterial fitness under antibiotic attack. We focused on the late stationary phase in which the intracellular ATP concentration displayed significant cell-to-cell heterogeneity (Fig. 1h). We monitored the intracellular ATP concentration and cell fate of QUEEN-7µ cells at 24 h stationary culture under 50 µg/mL (12.5 × minimum inhibitory concentration) ampicillin treatment for 240 min. The antibiotic killing and subsequent resuscitation were tracked in real-time at the single-cell level (Fig. 5a). Antibiotic treatment was carried out in fresh M9 medium supplemented with 1% glucose, while resuscitation was conducted in LB medium. According to their behavior, we categorized cells into three groups: "antibiotic-sensitive cells," undergoing lysis or being stained by PI during ampicillin treatment; "persisters," surviving antibiotic treatment and being resuscitated during LB incubation following antibiotic removal; and "VBNC cells," also surviving antibiotic treatment but remaining nonculturable during the 16 h LB incubation after antibiotic removal. As shown in Fig. 5a and b, these three groups of cells displayed distinct initial intracellular ATP concentrations prior to ampicillin treatment. Antibiotic-sensitive cells exhibited the highest mean intracellular ATP concentration, followed by persisters, while VBNC cells displayed the lowest (Fig. 5b and c). This observation aligns with previous research emphasizing the pivotal role of bacterial metabolic state in antibiotic lethality (42). Our study further delves into single-cell analysis, revealing that cells with higher intracellular ATP concentration are more prone to being antibiotic-sensitive by antibiotics. The overlap in ATP concentrations between antibiotic-sensitive cells and persisters suggests that factors other than ATP level may also influence cell states. It is generally believed that the VBNC and persister states represent two dormant phenotypes that span the spectrum between actively growing and non-viable cells. The intracellular ATP concentration of VBNC cells was found to be lower than that of persisters, suggesting that VBNC cells are in a deeper state of dormancy than persisters.

Remarkably, VBNC cells exhibited an intracellular ATP concentration lower than 32.5 µM in this experiment (Fig. 5e), which is consistent with that of VBNC cells by prolonged culture and indicates that these cells may have already entered the VBNC state prior to antibiotic treatment. Additionally, persisters displayed a relatively low intracellular ATP concentration ranging from 12.5 to 80 µM. Previous studies have suggested that persisters represent a transitory state leading to VBNC cells (21, 22), and the low intracellular ATP concentration in both VBNC and persister cells implies a close relationship between these two phenomena. Furthermore, an intracellular ATP concentration exceeding 80 µM led to cell death. We then investigated the dynamics of intracellular ATP concentration to further understand how it changes during antibiotic treatment (Fig. 5f and h). We found that VBNC cells maintained a low intracellular ATP concentration throughout antibiotic treatment, while the ATP concentration rapidly decreased in dead cells. In contrast, the intracellular ATP concentration of persisters fluctuated during antibiotic treatment. Taken together, these results highlight the relationship between intracellular ATP concentration and antibiotic tolerance. Antibiotic-tolerant persisters showing an intermediate intracellular ATP concentration were resuscitated, while cells with a high intracellular ATP concentration underwent cell death, and cells with an ultra-low intracellular ATP concentration remained non-resuscitative after antibiotic treatment. These findings suggest that bacterial cell fate during antibiotic treatment can be predicted simply by assessing the intracellular ATP concentration.

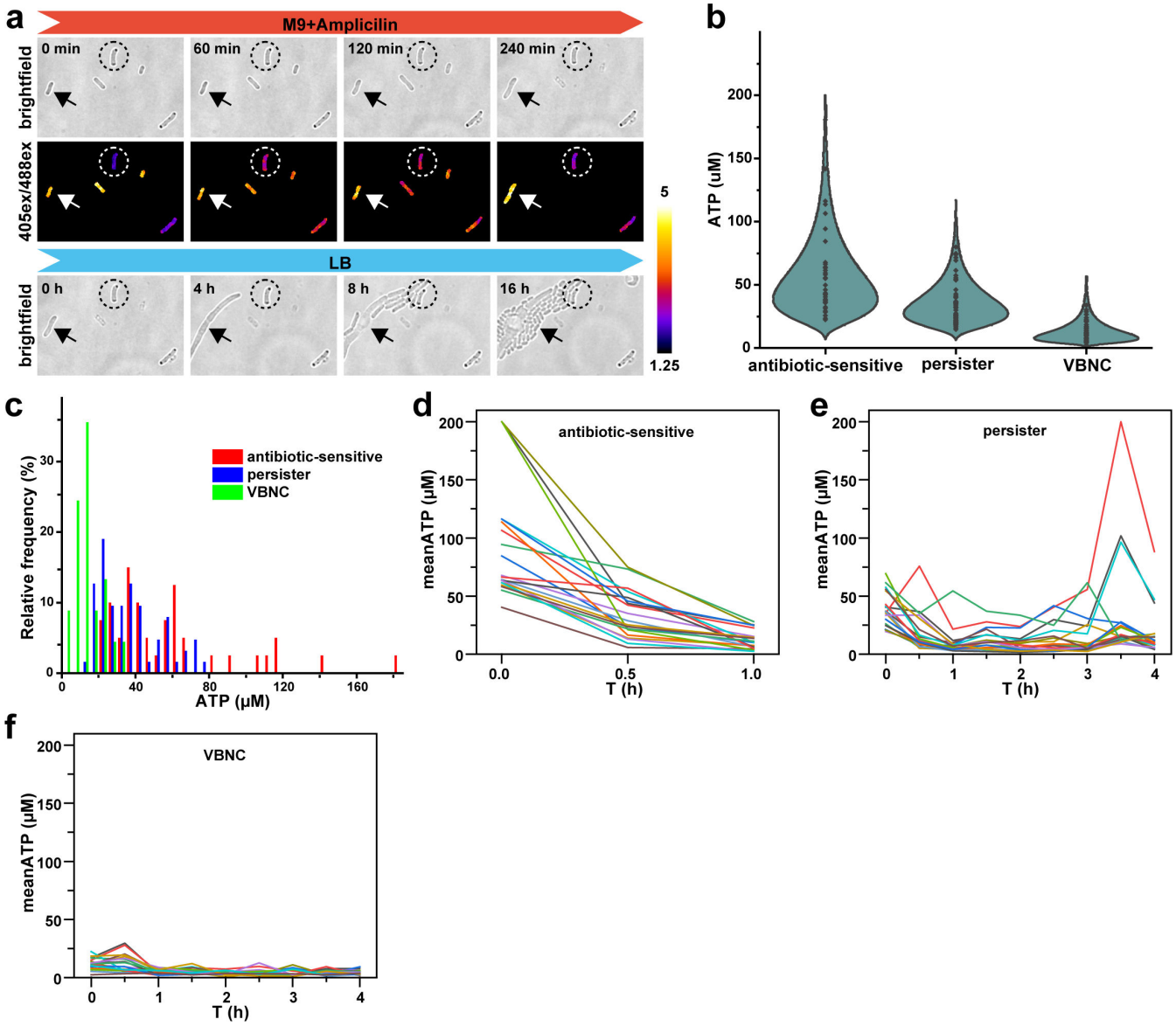

FIG 5 Role of the intracellular ATP concentration and heterogeneity in antibiotic tolerance. (a) Time-lapse images of QUEEN-7μ cells at 24 h stationary culture during ampicillin treatment and subsequent resuscitation. Time-lapse images represent the same field of view over time. Arrows indicate persister cells, while circles indicate VBNC cells. Scale bar, 5 μm. (b) Comparison of the intracellular ATP concentration among antibiotic-sensitive cells, persisters, and VBNC cells prior to ampicillin treatment. The distribution of the intracellular ATP concentration within each group is Log-normal estimated. (c) Intracellular ATP concentration distribution in antibiotic-sensitive cells, persisters, and VBNC cells prior to ampicillin treatment. (d–f) Dynamics of the intracellular ATP concentration in antibiotic-sensitive cells (d), persisters (e), and VBNC cells (f) during ampicillin treatment. A representative example of 20 cells selected at random illustrates dynamic changes in the intracellular ATP concentration. Error bars indicate SEM.

DISCUSSION

The VBNC and persister states are two dormant phenotypes characterized by low metabolic activity. At present, a significant challenge in addressing the VBNC phenomenon is the lack of precise identification and detection techniques, posing a considerable threat to food safety and public health (25). Following exposure to stress stimuli, VBNC cells undergo complex changes, including suppressed DNA replication, reduced macromolecular synthesis, increased oxidative stress, and membrane damage (8–11, 43–47). These changes are accompanied by a reduction in intracellular ATP concentration, establishing a physiological environment conducive to the formation of VBNC cells. To

investigate this phenomenon, we employed the single-cell ATP biosensor QUEEN-7μ to quantitate the intracellular ATP concentration of individual VBNC cells. Remarkably, we observed a significant decrease in the intracellular ATP concentration in VBNC cells and were able to identify a threshold of 12.5 μM that effectively distinguishes VBNC cells from their culturable counterparts. Utilizing FACS and this threshold, we successfully isolated VBNC cells from culturable cells, demonstrating the potential of the intracellular ATP concentration as a valuable indicator for the identification of individual VBNC cells.

Proteomic analysis suggests that protein precipitation, such as ribosome-associated proteins, may promote the formation of VBNC cells. Previous studies have reported a decrease in ribosome numbers within VBNC cells (48), accompanied by a notable reduction in the expression levels of ribosome-associated proteins compared to normal cells (49). We speculated that the observed increase in the abundance of ribosome-associated proteins in VBNC cells primarily results from ribosome disintegration or incomplete assembly, a phenomenon likely driven by the diminished intracellular ATP concentration. Additionally, ATP has also been reported to decrease the solubility of RNA-binding and ribosomal proteins (50, 51). Therefore, the decreased intracellular ATP concentration may be responsible for the release of a large number of ribosome-associated proteins observed in our study.

The most notable finding of the present study is that a substantial proportion of VBNC cells can be resuscitated after increasing the intracellular ATP concentration back to that of culturable cells. One of our previous studies already demonstrated that ATP-dependent protein aggregation can influence the depth of bacterial dormancy (18), and our present observations further establish a direct correlation between intracellular ATP levels and bacterial cell fate. Notably, cellular processes driven by ATP typically require ATP concentrations ranging from 10 to 500 μM (52); however, in culturable cells, the cytoplasmic ATP concentration is 10–100 times higher. Previous works have proposed that at a high concentration, ATP acts as a biological hydrotrope capable of preventing the formation of and dissolving protein aggregates (53, 54). Therefore, it can be inferred that during the early VBNC state, the decreased intracellular ATP concentration not only directly decelerates various cellular processes but also promotes protein precipitation. Conversely, elevating the intracellular ATP concentration accelerates cellular processes and facilitates the dissolution of precipitated proteins, resulting in a transformation of VBNC cells back to normal cells. We utilized PR in our experiments, which is prevalent in marine bacteria, to elevate the intracellular ATP concentration of *E. coli* cells. Our results imply that the strategy of increasing intracellular ATP concentration to resuscitate from VBNC states may potentially occur in the natural environment.

The growing concern over antibiotic therapy failure has inspired a surge in research on antibiotic persistence. Our persister-related findings emphasize the crucial role of intracellular ATP concentration in determining cell fate during antibiotic treatment. Specifically, persisters exhibited an intermediate intracellular ATP concentration, while cells with an intracellular ATP concentration exceeding 80 μM ultimately experienced cell death. This corroborates the protective role of slow growth, which shields bacteria from the bactericidal effects of many antibiotics. However, there is a significant overlap in ATP levels between antibiotic-sensitive cells and persisters, suggesting that ATP concentration alone does not strictly dictate cell fate during antibiotic exposure. Previous studies suggest that the expression of specific genes such as hipBA, TisB, TolC, hipBA, and ppGpp may be associated with the formation of persisters (55, 56).

Additionally, under antibiotic exposure, both VBNCs and persisters coexist, suggesting that persistence and the VBNC state are triggered by similar environmental stressors. This similarity underscores their relatedness. Moreover, the intracellular ATP concentrations of VBNC cells were found to be lower than those in persisters, indicating that VBNC cells are in a deeper state of dormancy. In contrast, persisters serve as a transitional state between antibiotic-sensitive and VBNC phenotypes (21). While various molecular mechanisms contribute to persister formation, our findings strongly suggest that decreased intracellular ATP concentration is a central physiological characteristic

associated with persistence. Considering these findings, it appears plausible to eradicate persisters by elevating their intracellular ATP concentration and subsequently employing conventional antibiotics to eliminate the reactivated cells.

Taken together, our findings highlight intracellular ATP concentration as a key regulator of bacterial cell fate, which provides a new perspective for understanding bacterial dormancy and holds potential for the development of new clinical treatment strategies against persisters and VBNC cells.

MATERIALS AND METHODS

Bacterial strains and plasmid construction

The wild-type strain used in this study was MG1655, which was kindly provided by the Yale Genetic Stock Center (CGSC#:6300). The plasmids essential for our experiments are listed in Table S1, and the corresponding primers used for subcloning are listed in Table S2. The pRSET::QUEEN-7μ and pET::proteorhodopsin plasmids were generously provided by Dr. Hideyuki Yaginuma and Dr. Qiong Wu, respectively. The proteorhodopsin PCR product was assembled into the pRSET::QUEEN-7μ plasmid using the *in vitro* Gibson assembly method. The resulting plasmids, pRSET::QUEEN-7μ, pET::proteorhodopsin, and pRSET::QUEEN-7μ-proteorhodopsin were introduced into MG1655 via electroporation. Subsequently, the transformed bacterial strains were cultured as follows: QUEEN-7μ and QUEEN-7μ-proteorhodopsin in LB medium supplemented with 25 μg/mL chloramphenicol, and the proteorhodopsin strain in LB medium containing 50 μg/mL kanamycin.

Reagents

Methionine, glutamine, threonine, serine, asparagine, catalase, and 50 × MEM amino acids solution were purchased from Sigma-Aldrich. Kanamycin, ampicillin, chloramphenicol, and other antibiotics were obtained from TransGen Biotech. The luminescent ATP detection assay kit employed in this study was acquired from Promega. D-2-deoxyglucose, an ATP depletion reagent, was bought from Sigma and sodium azide from Amresco. PI was obtained from Invitrogen, while PBS was purchased from Gibco. Unless otherwise stated, all other chemicals used in this study were procured from Sigma-Aldrich.

Purification and characterization of QUEEN-7μ

The QUEEN-7μ protein was purified from QUEEN-7μ *E. coli* cells cultured in LB medium following previously established protocols (32) and subsequently stored at −80°C. *In vitro* characterization of the protein was carried out using buffer C (50 mM HEPES, 200 mM KCl, 1 mM $MgCl_2$, and 0.05% Triton X-100) at 25°C. To assess the excitation spectra of QUEEN-7μ under varying ATP concentrations, a freshly prepared ATP stock solution was introduced into the protein solution to modify the ATP concentration. Once the solution stabilized, excitation was measured at wavelengths spanning 310–504 nm, with the emitted fluorescence recorded at 513 nm, utilizing a fluorescence spectrometer (F7000, Hitachi). To further investigate the relationship between the Ratio (405ex/488ex) of QUEEN-7μ and ATP concentration under the microscope, a 10 μg/mL purified QUEEN-7μ solution in buffer C at different ATP concentrations was injected into a channel formed by two coverslips separated by double-sided tape and subsequently imaged. The exposure time for 405 and 488 nm excitation was 200 and 150 ms, respectively. The fluorescence intensity of each channel was averaged from four different images, and the Ratio (405ex/488ex) was computed based on the mean values for each channel after background subtraction. Subsequently, we applied a Hill equation to fit the QUEEN-7μ calibration curve for Ratio (405ex/488ex), yielding a Kd of 17.5 μM.

Imaging

Brightfield and fluorescence imaging were conducted using a fluorescence microscope (Axio Observer Z1, Zeiss) equipped with a 100× oil-immersion objective (1.46 N.A.), an EMCCD camera (Evolve 512, Photometrics), and three different lasers: a 405 nm laser (OBIS405, Coherent) and a 488 nm laser (Sapphire 488, Coherent) for QUEEN-7μ imaging (ET525/50M), in addition to a 561 nm laser (Sapphire 561, Coherent) for PI imaging (ET605/70M). The microscope is also equipped with a Flow Cell System (FCS2, Bioptechs) for prolonged bacterial culture and time-lapse imaging. Prior to imaging, VBNC cells were sorted by flow cytometry (Aria SORP, BD), while late stationary phase cells were washed and resuspended in PBS. Subsequently, they were applied to a gel pad containing 3% low-melting temperature agarose, centrally located within the FCS2 chamber. Cells were imaged under both brightfield and fluorescence illumination at 25°C. To estimate the cellular ATP concentration using QUEEN-7μ, we imaged the cells with identical parameters to those employed for measuring the dose-response curve of purified QUEEN-7μ to ATP concentration. During the time-lapse imaging, the culture medium was injected into the chamber using an injection pump (LSP02-2B, LongerPump). The regrowth of late stationary phase cells or VBNC cells was recorded as movie files at 20 min per frame for 16 h.

Image processing

Custom MATLAB routines were employed for image analyses. Initially, cell segmentation was performed on the brightfield image, which was then converted into a binary image to facilitate the identification of intracellular and extracellular regions within the fluorescence image. For each channel and view, the images underwent background correction and removal of saturated pixels. Subsequently, the background-subtracted images were used to calculate the Ratio (405ex/488ex) for each individual cell, relying on the mean intensities of the respective channels. Cells displaying fluorescence intensities lower than the background in either channel were excluded from the data set. Given the minimal autofluorescence of wild-type MG1655 cells, no autofluorescence correction was applied during the experimental analysis. Finally, the Ratio of individual bacterial cells was converted into an ATP concentration by reference to the dose-response curve obtained using purified QUEEN-7μ.

Identification of VBNC and persister cells

VBNC cells represent a bacterial subpopulation that remains viable but does not undergo division on standard culture media, whereas persister cells exhibit phenotypic antibiotic tolerance. Here, the Flow Cell System FCS2 was utilized for prolonged bacterial culture and time-lapse imaging. To identify VBNC cells, late stationary phase *E. coli* cells or log-phase *E. coli* cells were subjected to various treatments: 20 μM $CuSO_4$ for 12 h, citric acid (pH 4.0) for 1 h, or cold shock at −20°C for 1 h. After the treatment, cells were washed and subsequently cultured in LB medium under a microscope. VBNC cells were identified by a lack of division following a 16 h incubation in LB medium. Additionally, PI staining was employed to exclude dead cells from the analysis. For the identification of persister cells, late stationary phase *E. coli* cells were treated with 50 μg/mL ampicillin for 240 min under a microscope. Following antibiotic treatment, cells were resuscitated by incubation in LB culture after the removal of the antibiotic. Persisters were identified among the surviving cells that were successfully resuscitated during LB incubation.

ATP measurement using the luciferase assay

The cellular ATP concentration of cells at 24 h stationary culture was quantitated using a commercially available BacTiter-Glo Microbial Cell Viability Assay Kit (Promega, G8231). Briefly, after 24 h of culture, QUEEN-7μ cells were washed and resuspended in PBS, and then 100 μL cell suspension and 100 μL reagent from the kit were combined in an opaque-walled 96-well plate. The plate was incubated on an orbital shaker for 5 min,

and the luminescence was promptly measured using a multi-mode microplate reader (Cytation5, BioTek). The luminescence intensity indicated the intracellular ATP concentration, which was normalized based on the cell number and single-cell column. Determination of cell number and cell volume was accomplished by brightfield imaging. For each experimental setup, including the blank and experimental groups, quadruplicate samples were established. To account for background noise, the mean value of the blank group was subtracted from the recorded luminescence values.

Flow cytometry and cell sorting

Flow cytometry and cell sorting were conducted using a BD FACSAria SORP Cell Sorter. Prior to cell sorting, the Ratio (405ex/488ex) distribution of QUEEN-7μ cells at 30 h stationary culture was measured by flow cytometry. Briefly, QUEEN-7μ cells were washed and resuspended in PBS after 30 h of LB culture. After staining with PI for 15 min, the cell suspension was carefully filtered into a FACS tube (BD) for further flow cytometry analysis. PI fluorescence, serving as an indicator of cell viability, was excited using a 561 nm laser and collected through a 610/20 band-pass filter (PE channel). Simultaneously, the green fluorescence emitted by QUEEN-7μ, excited by both the 405 and 488 nm lasers, was collected through a 530/30 band-pass filter (V500 and FITC channel). Flow cytometry data were analyzed using the FlowJo v10.8 Software (BD Life Sciences). Following the exclusion of PI+ cells, the Ratio of QUEEN-7μ cells was calculated based on the fluorescence intensities recorded in the V500-A and FITC-A channels. After flow cytometry analysis, cell sorting was conducted by implementing the sequential gating strategies as illustrated in Fig. S3, employing a 70 μm nozzle. Single cells were identified based on their side and forward scatter areas. Live cells were distinguished by their PI fluorescence intensity. QUEEN-7μ+ cells were gated using the fluorescence intensity observed in both the V500-A and FITC-A channels to eliminate cells with low fluorescence intensities. Finally, VBNC and culturable cells were gated based on the Ratio (V500-A/FITC-A). A constant rate of 10,000 events/s was maintained during cell sorting. After sorting, cells were centrifuged at 10,000 × *g* for 5 min and resuspended in PBS for subsequent imaging and proteome analysis.

Isolation of the soluble and insoluble proteomes

The method used to isolate the soluble and insoluble proteomes from VBNC and culturable cells was adapted from Tomoyasu et al. (57). Briefly, VBNC and culturable cells, sorted by FACS, were rapidly cooled on ice and subjected to centrifugation at 10,000 × *g* (4°C) for 5 min to remove the culture media. Subsequently, cells were resuspended in 40 μL buffer A (10 mM potassium phosphate buffer, pH 6.5, 1 mM EDTA, and 0.1 μg/μL lysozyme) and incubated on ice for 30 min. Following the incubation, sonication was carried out for 30 min at 4°C to disrupt the cells, and intact cells were removed from the lysate by centrifugation at 2,000 × *g* (4°C) for 2 min. The supernatant, which contained the soluble proteome, was isolated by centrifugation at 15,000 × *g* (4°C) for 20 min, while the insoluble proteome remained in the pellet. The pellet fraction was then resuspended in 1,000 μL buffer C (10 mM potassium phosphate buffer, pH 6.5, 1 mM EDTA, and 2% NP40) to dissolve membrane proteins. Additional sonification (30 min) and centrifugation (15,000 × *g*, 20 min, 4°C) were carried out to isolate the insoluble proteome. The NP40-insoluble pellet was washed with 1,000 μL buffer B (10 mM potassium phosphate buffer, pH 6.5, and 1 mM EDTA) and resuspended in 40 μL buffer B through brief sonification. Finally, the soluble and insoluble proteomes were analyzed by 12% SDS-PAGE and stained with Coomassie brilliant blue.

GO enrichment analysis

Prior to conducting GO enrichment analysis, the R package clusterProfiler (v3.13) and R studio (v4.1.1) software were used to convert the protein identifiers obtained from protein mass spectrometry analysis to their corresponding gene identifiers in

the Kyoto Encyclopedia of Genes and Genomes database. Subsequently, the significantly increased insoluble proteome, significantly decreased soluble proteome, and significantly increased soluble proteome were identified in VBNC cells in comparison with culturable cells. This identification was based on the ratio of relative cumulative peptide intensities, with the threshold set at ≥2 (≤0.5). Finally, GO enrichment analysis was conducted on these proteome data sets using the clusterProfiler package and the enrichGO function, encompassing assessments of biological processes, molecular functions, and cellular components.

Resuscitation assay

To eliminate the potential influence of cell proliferation, the resuscitation assay was conducted using either agar plates or non-nutritive PBS medium. For resuscitation assays involving amino acids and catalase, 100 µL FACS-sorted VBNC cells were mixed with 100 µL resuscitation reagent and evenly spread onto LB agar plates. The resuscitation reagents included catalase (5 U/µL), 1 × MEM amino acids solution, and a specific combination of amino acids (40 µg/mL each methionine, glutamine, threonine, serine, and asparagine) (35). In the resuscitation assay by ATP elevation, QUEEN-7µ-PR cells at 30 h stationary culture were washed, resuspended in PBS, and then incubated in a shaker (200 rpm) at 37°C in the presence or absence of 2 mW green light illumination. To minimize the potential impact of light, the green light was cycled for 5 min on and 35 min off. Additionally, 20 µM all-*trans* retinal was introduced during the resuscitation assay. After a specific period of illumination, 10 µL bacterial samples were collected, diluted in PBS buffer, and subsequently plated onto LB agar plates for overnight culture at 37°C. After 24 h, colony-formation unit (CFU) counting was performed. The ratio of culturable cells was determined by dividing the CFU count by the number of FACS-sorted cells. The increase in ratio of culturable cells after adding amino acid or catalase was defined as the resuscitation ratio. Each experiment was carried out in triplicate.

ACKNOWLEDGMENTS

We thank Dr. Hideyuki Yaginuma (The University of Tokyo) for providing the pRSET::QUEEN-7µ plasmid and Dr. Qiong Wu (Tsinghua University) for providing the pET::proteorhodopsin plasmid. We thank the National Center for Protein Sciences at Peking University in Beijing, China for assistance with mass spectrometry and Qi Zhang for her help with MS data analysis. We also thank Bin Yu (Core Facility, Center of Biomedical Analysis, Tsinghua University) for technical support with flow cytometry analysis.

This work was financially supported by the National Science Fund for Distinguished Young Scholars (T2125002).

B.L. and F.B. conceived the project. B.L., X.C., J.Y., and S.G. performed the experiments. B.L. analyzed and interpreted the data. B.L. and F.B. wrote the paper. F.B. supervised the project. All authors edited and approved the paper.

AUTHOR AFFILIATIONS

[1]Biomedical Pioneering Innovation Center (BIOPIC), Beijing Advanced Innovation Center for Genomics (ICG), School of Life Sciences, Peking University, Beijing, China
[2]State Key Laboratory of Oncology in South China, Collaborative Innovation Center for Cancer Medicine, Sun Yat-Sen University Cancer Center, Guangzhou, Guangdong, China

AUTHOR ORCIDs

Bo Li http://orcid.org/0009-0004-0852-1000
Fan Bai http://orcid.org/0000-0001-6119-8936

DATA AVAILABILITY

All data needed to evaluate the conclusions in the paper are present in the paper and the supplementary materials. Any additional requests for information can be directed to, and will be fulfilled by, the corresponding authors.

ADDITIONAL FILES

The following material is available online.

Supplemental Material

Supplemental figures and tables (JB00208-24-s0001.docx). Fig. S1 to S8, Table S1 and S2, and Supplemental movie legends.
pRSET::QUEEN-7µ vector (JB00208-24-s0002.txt). Sequence details of the pRSET::QUEEN-7µ-proteorhodopsin plasmid.
Table S3 (JB00208-24-s0003.xlsx). Soluble and insoluble proteomes in VBNC and culturable cells.
Movie S1 (JB00208-24-s0004.avi). Resuscitation of QUEEN-7µ cells at 30 h stationary culture with fresh LB medium incubation.
Movie S2 (JB00208-24-s0005.avi). Sorted VBNC cells showed no signs of resuscitation upon incubation in fresh LB medium.
Movie S3 (JB00208-24-s0006.avi). Resuscitation of sorted culturable cells observed during extended LB culture under a microscope.

REFERENCES

1. Cook KL, Bolster CH. 2007. Survival of *Campylobacter jejuni* and *Escherichia coli* in groundwater during prolonged starvation at low temperatures. J Appl Microbiol 103:573–583. https://doi.org/10.1111/j.1365-2672.2006.03285.x
2. Wu B, Liang W, Yan M, Li J, Zhao H, Cui L, Zhu F, Zhu J, Kan B. 2020. Quorum sensing regulation confronts the development of a viable but non-culturable state in *Vibrio cholerae*. Environ Microbiol 22:4314–4322. https://doi.org/10.1111/1462-2920.15026
3. Salive AFV, Prudêncio CV, Baglinière F, Oliveira LL, Ferreira SO, Vanetti MCD. 2020. Comparison of stress conditions to induce viable but non-cultivable state in *Salmonella*. Braz J Microbiol 51:1269–1277. https://doi.org/10.1007/s42770-020-00261-w
4. Besnard V, Federighi M, Declerq E, Jugiau F, Cappelier JM. 2002. Environmental and physico-chemical factors induce VBNC state in *Listeria monocytogenes*. Vet Res 33:359–370. https://doi.org/10.1051/vetres:2002022
5. Xu HS, Roberts N, Singleton FL, Attwell RW, Grimes DJ, Colwell RR. 1982. Survival and viability of nonculturable *Escherichia coli* and *Vibrio cholerae* in the estuarine and marine environment. Microb Ecol 8:313–323. https://doi.org/10.1007/BF02010671
6. Alleron L, Khemiri A, Koubar M, Lacombe C, Coquet L, Cosette P, Jouenne T, Frere J. 2013. VBNC *Legionella pneumophila* cells are still able to produce virulence proteins. Water Res 47:6606–6617. https://doi.org/10.1016/j.watres.2013.08.032
7. Ducret A, Chabalier M, Dukan S. 2014. Characterization and resuscitation of 'non-culturable' cells of *Legionella pneumophila*. BMC Microbiol 14:3. https://doi.org/10.1186/1471-2180-14-3
8. Trevors JT. 2011. Viable but non-culturable (VBNC) bacteria: gene expression in planktonic and biofilm cells. J Microbiol Methods 86:266–273. https://doi.org/10.1016/j.mimet.2011.04.018
9. Rozen Y, Larossa RA, Templeton LJ, Smulski DR, Belkin S. 2002. Gene expression analysis of the response by *Escherichia coli* to seawater. Antonie Van Leeuwenhoek 81:15–25. https://doi.org/10.1023/a:1020500821856
10. Muela A, Seco C, Camafeita E, Arana I, Orruño M, López JA, Barcina I. 2008. Changes in *Escherichia coli* outer membrane subproteome under environmental conditions inducing the viable but nonculturable state. FEMS Microbiol Ecol 64:28–36. https://doi.org/10.1111/j.1574-6941.2008.00453.x
11. Jeffreys AG, Hak KM, Steffan RJ, Foster JW, Bej AK. 1998. Growth, survival and characterization of *cspA* in *Salmonella enteritidis* following cold shock. Curr Microbiol 36:29–35. https://doi.org/10.1007/s002849900275
12. Lewis K. 2010. Persister cells. Annu Rev Microbiol 64:357–372. https://doi.org/10.1146/annurev.micro.112408.134306
13. Zhang Y, Yew WW, Barer MR. 2012. Targeting persisters for tuberculosis control. Antimicrob Agents Chemother 56:2223–2230. https://doi.org/10.1128/AAC.06288-11
14. Sharma B, Brown AV, Matluck NE, Hu LT, Lewis K. 2015. *Borrelia burgdorferi*, the causative agent of Lyme disease, forms drug-tolerant persister cells. Antimicrob Agents Chemother 59:4616–4624. https://doi.org/10.1128/AAC.00864-15
15. Ayrapetyan M, Williams TC, Baxter R, Oliver JD. 2015. Viable but nonculturable and persister cells coexist stochastically and are induced by human serum. Infect Immun 83:4194–4203. https://doi.org/10.1128/IAI.00404-15
16. Maisonneuve E, Gerdes K. 2014. Molecular mechanisms underlying bacterial persisters. Cell 157:539–548. https://doi.org/10.1016/j.cell.2014.02.050
17. Wang X, Wood TK. 2011. Toxin-antitoxin systems influence biofilm and persister cell formation and the general stress response. Appl Environ Microbiol 77:5577–5583. https://doi.org/10.1128/AEM.05068-11
18. Pu Y, Li Y, Jin X, Tian T, Ma Q, Zhao Z, Lin S-Y, Chen Z, Li B, Yao G, Leake MC, Lo C-J, Bai F. 2019. ATP-dependent dynamic protein aggregation regulates bacterial dormancy depth critical for antibiotic tolerance. Mol Cell 73:143–156. https://doi.org/10.1016/j.molcel.2018.10.022
19. Manuse S, Shan Y, Canas-Duarte SJ, Bakshi S, Sun WS, Mori H, Paulsson J, Lewis K. 2021. Bacterial persisters are a stochastically formed subpopulation of low-energy cells. PLoS Biol 19:e3001194. https://doi.org/10.1371/journal.pbio.3001194
20. Balaban NQ, Merrin J, Chait R, Kowalik L, Leibler S. 2004. Bacterial persistence as a phenotypic switch. Science 305:1622–1625. https://doi.org/10.1126/science.1099390
21. Ayrapetyan M, Williams TC, Oliver JD. 2015. Bridging the gap between viable but non-culturable and antibiotic persistent bacteria. Trends Microbiol 23:7–13. https://doi.org/10.1016/j.tim.2014.09.004

22. Bamford RA, Smith A, Metz J, Glover G, Titball RW, Pagliara S. 2017. Investigating the physiology of viable but non-culturable bacteria by microfluidics and time-lapse microscopy. BMC Biol 15:121. https://doi.org/10.1186/s12915-017-0465-4
23. Ayrapetyan M, Williams T, Oliver JD, Margolin W. 2018. Relationship between the viable but nonculturable state and antibiotic persister cells. J Bacteriol 200:e00249-18. https://doi.org/10.1128/JB.00249-18
24. Orman MA, Brynildsen MP. 2013. Establishment of a method to rapidly assay bacterial persister metabolism. Antimicrob Agents Chemother 57:4398–4409. https://doi.org/10.1128/AAC.00372-13
25. Shamloei S, Nabavi-Rad A, Nazem H, Yadegar A. 2022. Current perspectives on viable but non-culturable bacteria in food safety and public health. Avicenna J Clin Microbiol Infect 9:31–40. https://doi.org/10.34172/ajcmi.2022.06
26. Li Y, Chen J, Zhao M, Yang Z, Yue L, Zhang X. 2017. Promoting resuscitation of viable but nonculturable cells of *Vibrio harveyi* by a resuscitation-promoting factor-like protein YeaZ. J Appl Microbiol 122:338–346. https://doi.org/10.1111/jam.13342
27. Ayrapetyan M, Williams TC, Oliver JD. 2014. Interspecific quorum sensing mediates the resuscitation of viable but nonculturable vibrios. Appl Environ Microbiol 80:2478–2483. https://doi.org/10.1128/AEM.00080-14
28. Alleron L, Merlet N, Lacombe C, Frère J. 2008. Long-term survival of *Legionella pneumophila* in the viable but nonculturable state after monochloramine treatment. Curr Microbiol 57:497–502. https://doi.org/10.1007/s00284-008-9275-9
29. Schwiebert EM, Zsembery A. 2003. Extracellular ATP as a signaling molecule for epithelial cells. Biochim Biophys Acta 1615:7–32. https://doi.org/10.1016/s0005-2736(03)00210-4
30. Patel A, Malinovska L, Saha S, Wang J, Alberti S, Krishnan Y, Hyman AA. 2017. ATP as a biological hydrotrope. Science 356:753–756. https://doi.org/10.1126/science.aaf6846
31. Conlon BP, Rowe SE, Gandt AB, Nuxoll AS, Donegan NP, Zalis EA, Clair G, Adkins JN, Cheung AL, Lewis K. 2016. Persister formation in *Staphylococcus aureus* is associated with ATP depletion. Nat Microbiol 1:16051. https://doi.org/10.1038/nmicrobiol.2016.51
32. Yaginuma H, Kawai S, Tabata KV, Tomiyama K, Kakizuka A, Komatsuzaki T, Noji H, Imamura H. 2014. Diversity in ATP concentrations in a single bacterial cell population revealed by quantitative single-cell imaging. Sci Rep 4:6522. https://doi.org/10.1038/srep06522
33. Lin W-H, Jacobs-Wagner C. 2022. Connecting single-cell ATP dynamics to overflow metabolism, cell growth, and the cell cycle in *Escherichia coli*. Curr Biol 32:3911–3924. https://doi.org/10.1016/j.cub.2022.07.035
34. Cranfill PJ, Sell BR, Baird MA, Allen JR, Lavagnino Z, de Gruiter HM, Kremers G-J, Davidson MW, Ustione A, Piston DW. 2016. Quantitative assessment of fluorescent proteins. Nat Methods 13:557–562. https://doi.org/10.1038/nmeth.3891
35. Pinto D, Almeida V, Almeida Santos M, Chambel L. 2011. Resuscitation of *Escherichia coli* VBNC cells depends on a variety of environmental or chemical stimuli. J Appl Microbiol 110:1601–1611. https://doi.org/10.1111/j.1365-2672.2011.05016.x
36. Nandi A, Yan LJ, Jana CK, Das N. 2019. Role of catalase in oxidative stress- and age-associated degenerative diseases. Oxid Med Cell Longev 2019:9613090. https://doi.org/10.1155/2019/9613090
37. Ighodaro OM, Akinloye OA. 2018. First line defence antioxidants-superoxide dismutase (SOD), catalase (CAT) and glutathione peroxidase (GPX): their fundamental role in the entire antioxidant defence grid. Alex J Med 54:287–293. https://doi.org/10.1016/j.ajme.2017.09.001
38. Liu J, Li L, Li B, Peters BM, Deng Y, Xu Z, Shirtliff ME. 2017. Study on spoilage capability and VBNC state formation and recovery of *Lactobacillus plantarum*. Microb Pathog 110:257–261. https://doi.org/10.1016/j.micpath.2017.06.044
39. Béjà O, Aravind L, Koonin EV, Suzuki MT, Hadd A, Nguyen LP, Jovanovich SB, Gates CM, Feldman RA, Spudich JL, Spudich EN, DeLong EF. 2000. Bacterial rhodopsin: evidence for a new type of phototrophy in the sea. Science 289:1902–1906. https://doi.org/10.1126/science.289.5486.1902
40. Martinez A, Bradley AS, Waldbauer JR, Summons RE, DeLong EF. 2007. Proteorhodopsin photosystem gene expression enables photophosphorylation in a heterologous host. Proc Natl Acad Sci USA 104:5590–5595. https://doi.org/10.1073/pnas.0611470104
41. Béjà O, Spudich EN, Spudich JL, Leclerc M, DeLong EF. 2001. Proteorhodopsin phototrophy in the ocean. Nat New Biol 411:786–789. https://doi.org/10.1038/35081051
42. Lopatkin AJ, Stokes JM, Zheng EJ, Yang JH, Takahashi MK, You L, Collins JJ. 2019. Bacterial metabolic state more accurately predicts antibiotic lethality than growth rate. Nat Microbiol 4:2109–2117. https://doi.org/10.1038/s41564-019-0536-0
43. Noor R. 2015. Mechanism to control the cell lysis and the cell survival strategy in stationary phase under heat stress. Springerplus 4:599. https://doi.org/10.1186/s40064-015-1415-7
44. Fu Y, Jia Y, Fan J, Yu C, Yu C, Shen C. 2020. Induction of *Escherichia coli* O157: H7 into a viable but non-culturable state by high temperature and its resuscitation. Environ Microbiol Rep 12:568–577. https://doi.org/10.1111/1758-2229.12877
45. Nyström T. 2001. Not quite dead enough: on bacterial life, culturability, senescence, and death. Arch Microbiol 176:159–164.
46. Se J, Fu Y, Xie Y, Xu F, Shen C, Nannipieri P. 2021. Proteomic changes of viable but nonculturable (VBNC) *Escherichia coli* O157:H7 induced by low moisture in an artificial soil. Biol Fertil Soils 57:219–234. https://doi.org/10.1007/s00374-020-01520-6
47. Cuny C, Dukan L, Fraysse L, Ballesteros M, Dukan S. 2005. Investigation of the first events leading to loss of culturability during *Escherichia coli* starvation: future nonculturable bacteria form a subpopulation. J Bacteriol 187:2244–2248. https://doi.org/10.1128/JB.187.7.2244-2248.2005
48. Zhao F, Bi X, Hao Y, Liao X. 2013. Induction of viable but nonculturable *Escherichia coli* O157:H7 by high pressure CO2 and its characteristics. PLoS ONE 8:e62388. https://doi.org/10.1371/journal.pone.0062388
49. Ramamurthy T, Ghosh A, Pazhani GP, Shinoda S. 2014. Current perspectives on viable but non-culturable (VBNC) pathogenic bacteria. Front Public Health 2:103. https://doi.org/10.3389/fpubh.2014.00103
50. Sridharan S, Kurzawa N, Werner T, Günthner I, Helm D, Huber W, Bantscheff M, Savitski MM. 2019. Proteome-wide solubility and thermal stability profiling reveals distinct regulatory roles for ATP. Nat Commun 10:1155. https://doi.org/10.1038/s41467-019-09107-y
51. Piazza I, Kochanowski K, Cappelletti V, Fuhrer T, Noor E, Sauer U, Picotti P. 2018. A map of protein-metabolite interactions reveals principles of chemical communication. Cell 172:358–372. https://doi.org/10.1016/j.cell.2017.12.006
52. Rice AM, Rosen MK. 2017. ATP controls the crowd. Science 356:701–702. https://doi.org/10.1126/science.aan4223
53. Munder MC, Midtvedt D, Franzmann T, Nüske E, Otto O, Herbig M, Ulbricht E, Müller P, Taubenberger A, Maharana S, Malinovska L, Richter D, Guck J, Zaburdaev V, Alberti S. 2016. A pH-driven transition of the cytoplasm from a fluid- to a solid-like state promotes entry into dormancy. Elife 5:e09347. https://doi.org/10.7554/eLife.09347
54. Kang J, Lim L, Song J. 2019. ATP binds and inhibits the neurodegeneration-associated fibrillization of the FUS RRM domain. Commun Biol 2:223. https://doi.org/10.1038/s42003-019-0463-x
55. Keren I, Shah D, Spoering A, Kaldalu N, Lewis K. 2004. Specialized persister cells and the mechanism of multidrug tolerance in *Escherichia coli*. J Bacteriol 186:8172–8180. https://doi.org/10.1128/JB.186.24.8172-8180.2004
56. Dörr T, Vulić M, Lewis K. 2010. Ciprofloxacin Causes Persister Formation by Inducing the TisB toxin in *Escherichia coli*. PLoS Biol 8:e1000317. https://doi.org/10.1371/journal.pbio.1000317
57. Tomoyasu T, Mogk A, Langen H, Goloubinoff P, Bukau B. 2001. Genetic dissection of the roles of chaperones and proteases in protein folding and degradation in the *Escherichia coli* cytosol. Mol Microbiol 40:397–413. https://doi.org/10.1046/j.1365-2958.2001.02383.x